Analog Optical Signal Processing of Baseband Codes in Tm:YAG up to 10 Gb/s

Kristian D. Merkel, R. Krishna Mohan, Zachary Cole, Randy R. Reibel,
Todd L. Harris, Tiejun Chang and W. Randall Babbitt
Spectrum Lab, Montana State University, P.O. Box 173510, Bozeman, MT 59717

Abstract-**Aspects of analog signal processing are explored using baseband codes from 1 to 10 Gb/s modulated onto a 378 THz optical carrier and processed by spectral holographic techniques in Tm:YAG. Results include processing of signals buried in additive noise, variation of time delays over 5 μs, and material signal losses as low as ~1 dB/μs.**

Index Terms—**Analog Optical Signal Processing, Radar Signal Processing, Spatial-Spectral Holography, Optical coherent transients**

I. Introduction

THE spectral diversity of radar, communications and electronic warfare continues to expand, as systems employ complex coding and multiplexing schemes to make better use of the bandwidths allocated to them. With the use of complex digital modulation, spectral allocation is becoming more dynamic as signals continually change carriers, formats and bandwidths depending upon needs. As the use of the radio frequency spectrum evolves, there is a need for signal processing systems that can perform with large dynamic range in real-time over wide bandwidths. While analog to digital converters (ADCs) are achieving widespread use in receiver chains and move closer to the antenna, they suffer in performance at higher sample rates. In a 1999 survey [1], Walden showed that the performance of ADCs falls off at a rate of ~1 dB per octave of bandwidth. This trend has not seen significant improvement in recent years, as Walden predicted, despite active research in new material work, such as in SiGe, with a typical specification of 3-bits at 20 to 40 Gs/s [2,3]. Along with the limitations of ADCs, in order to process the captured information at such high sample rates, digital signal processor technology will need to scale to achieve real time operation. These factors represent a significant research challenge and present limitations for consideration of using wide bandwidth waveforms in real-time digital signal processing systems.

For these reasons, photonic approaches to performing a range of analog signal processing functions are attractive. One such analog optical signal processor (AOSP) has the ability to meet the needs of broadband, high dynamic range, real time processing, based upon the ultrawide absorption response of narrow linewidth rare earth ions doped into crystalline materials (e.g., inhomogeneously broadened transitions). This type of AOSP can actively process wideband signals to determine delays between waveforms (range processing), as well as coherently integrate multiple results to increase the signal-to-noise and determine frequency shifts between waveforms (Doppler processing).

In this paper, we discuss multiple core aspects of an analog optical signal processor utilizing the 378.13 THz optical transition ($^3H_4$ to $^3H_6$) in a cryogenically cooled Tm:YAG sample at 4K. In this work a baseband coding scheme was employed to demonstrate device capabilities, such as: a) coherent processing of large time-bandwidth product analog signals in noisy environments, b) the integration of multiple processing results, c) operation over a substantial ~5 μs time-aperture while maintaining significant signal-to-noise ratios, d) meeting a performance implementation loss criterion of ~1 dB/μs over this time-aperture, and e) processing of baseband codes with data rates up to 10 Gb/s.

II. Background on S2 Analog Optical Processing

The basic operation of the analog optical processor is the recording of a spatial spectral (S2) interference pattern as a holographic grating within the absorbing transition. Typically an S2 interference grating is created by a pair of optical fields that are both temporally distinct and angularly separated. For two identical but delayed temporally brief plane waves, the result is a spectral grating with a period that is inversely proportional to the time delay between the fields, and a spatial grating that is inversely proportional to the wave-vector difference of the propagation directions. For complex fields, this operation can be used to process and integrate radar return signals for range-Doppler processing, for triangulation of the same received signal at different time delays between two antennas, or to search for an expected return from a library reference of signatures, as well as other applications [4,5].

In the implementation of this device, coded RF signals are modulated onto a stable optical carrier, which irradiates the material. The material responds to the power spectrum of the combined electric fields over the coherent time-aperture of the

This work was supported in part by the Montana Board of Research and Commercialization of Technology (MBRCT) under grant Z4193 and by the Defense Advanced Research Projects Agency (DARPA) under grant MDA972-03-1-0002. Dr. Merkel's can be reached by email at merkel@spectrum.montana.edu, phone 406-994-7241 or fax 406-994-6767.

material, resulting in atomic transitions that store and record the power spectrum as S2 holographic grating. The integration of multiple such exposures over the persistence time of the atomic transition can strengthen the grating signature. The RF signal is encoded onto the optical carrier through the use of electro-optic phase modulators (EOPMs), which change the optical carrier phase in proportion to the sign and magnitude of the applied RF voltage. Two EOPMs may be used, one for the reference waveform and one for the signal waveform, where the light from each is made to overlap in the S2 material at a small angle.

Within the persistence time of the transition, the S2 grating can be continuously probed with an appropriate readout waveform. An apparatus to create an optical frequency chirped pulse can be used to readout the spectral grating by making a temporal map of the grating spectral structure. In this case, a broadband optical chirp can be created by a number of means, including using acousto-optic modulators or electro-optic modulators driven with a chirped RF source [6], or by utilizing a piezo-electric or intracavity electro-optic material to change the cavity length of a laser [7]. A desirable optical chirped pulse has a linear variation in its carrier frequency at a chirp rate $\kappa=B_{ch}/T_{ch}$ over a bandwidth B_{ch} over a duration T_{ch}. Ultimately, T_{ch} is limited by the material persistence time, placing a lower limit on κ for a given B_{ch}.

Physically, the input chirped readout pulse interacts with the spectral grating, stimulating the emission of photon echo fields as delayed replicas of the readout pulse. This output field can be made to interfere with a suitable reference chirped waveform, providing beat frequencies that are directly proportional to the time delays. In an angled processing geometry, this echo signal will be spatially distinct from the transmitted readout pulse, providing the capability to use a reference chirped waveform that is not affected by transmission through the absorbing material [8].

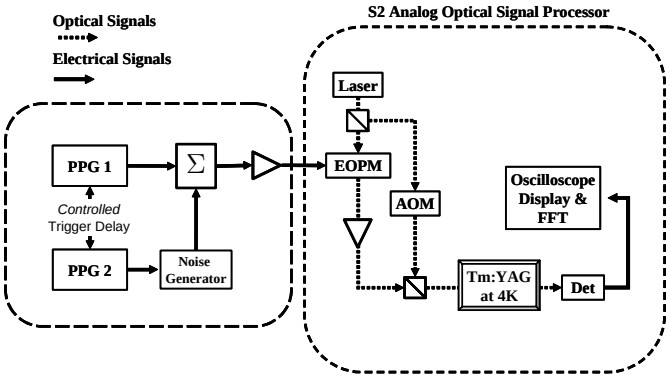

Fig. 1. Experimental setup for baseband demonstrations from 1 to 10 Gb/s. Two pulse pattern generators (PPG 1 and PPG2) were synchronized with a controllable trigger delay. The signal from PPG2 could be attenuated and have additive noise. These signals were combined and applied to the EOPM, creating a modulated optical carrier, which was applied to the Tm:YAG sample. An AOM was used to create a readout waveform, applied collinearly to the sample, which was detected and digitized.

The practicality in this approach comes from the fact that the readout signal provides a wideband temporal mapping of the S2 grating (high bandwidth processing results) as a reduced bandwidth signal, essentially making it possible to perform optical-to-electrical conversion and electrical analog-to-digital conversion at a significantly reduced bandwidth with large dynamic range (e.g. 14 bits at 100 Ms/s).

III. Background for Experiemental Work

A. Experimental Setup

The experimental setup used is shown in Figure 1. The master optical oscillator was a frequency stabilized Ti:Sapphire laser, locked to a regenerative spectral hole frequency reference [9]. Two pulse pattern generators (PPGs) were used to generate digital binary codes that were subsequently summed, amplified and fed to an EOPM. Each

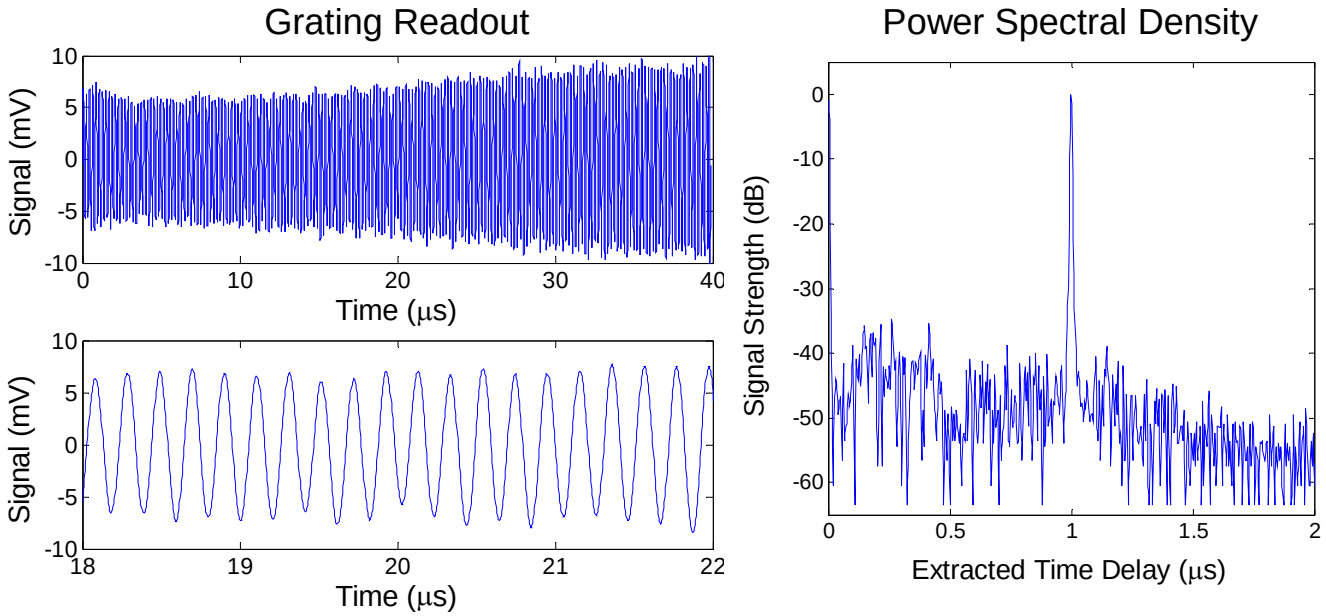

Fig. 2. Typical data set of spectral grating readout using chirped optical pulses (left). The readout chirped pulse was created by an AOM (double passed) over 200 MHz in 40 μs (chirp rate of ~5 MHz/μs, 1 μs delay). The power spectral density (right) of the top left trace shows the processing result at a delay of 1 μs, with ~42 dB peak-to-rms sidelobe ratio measured over 0.5 to 1.0 μs.

PPG was programmed with an identical 8 MB sequence consisting of pseudo-random noise (PN) patterns, each with a duration of 512 ns and a repetition frequency of 100 kHz (e.g. a new PN code generated every 10 μs). The time delay between a pattern and its replica were controlled via the PPG internal oscillators. The modulated optical output of the EOPM (~1 mW) was amplified by injection locking of a high power diode laser [10]. This light could be further optically amplified to ~300 mW with a semiconductor optical amplifier. This light was made to irradiate a volume of a Tm:YAG sample held at 4K (100 μm diameter beam measured at 1/e intensity drop, over the sample length).

The readout pulse for probing the recorded spectral grating was either an optical chirp of 200 MHz in 40 μs, or a 50 ns brief pulse. In both cases, this waveform was generated by an acousto-optic modulator (AOM) driven by an arbitrary waveform generator. The readout light was collinearly applied to the volume, then photo-detected and digitized.

B. Signal extraction by chirped readout

A typical result of the chirped readout technique is shown in Figure 2 (left), after the material had been irradiated by 750 shots of PN sequences modulated at 1 Gb/s (512 bit codes). Here the spectral grating is mapped into the time domain, where the periodicity of the spectral structure, which is inversely related to the 1 μs time delay between the input pulse pairs, is observed. A plot of the power spectral density (right) of the sinusoidal structure yields frequency information, that when scaled by the chirp rate, yields the time delays.

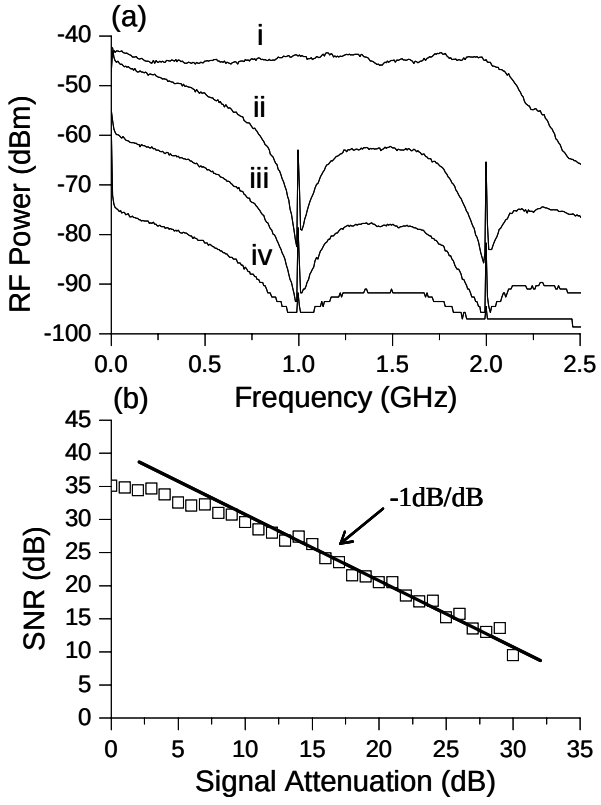

Fig. 3. Demonstration of processing attenuated signals in noise. (a) RF spectrum analyzer traces (RBW=30 kHz) of input sequences for experimental demonstrations of signal extraction in the presence of noise, before the RF amplifier. Trace (i) shows broadband noise and traces (ii)-(iv) show return signal spectra at various levels of attenuation, without noise being added. (b) The processed output SNR as a function of the return signal attenuation, when the noise in (i) was summed with the signals such as those in (ii)-(iv) at various attenuation levels from 0 to 30 dB. A 1 dB/dB drop in the SNR is observed for small signals.

IV. 1.0 GB/S SIGNALS ATTENUATED AND BURIED IN NOISE

In a radar application, the antenna receives the scattered target signal that is attenuated and buried in noise. Proof of concept experiments were performed to test the ability of the Tm:YAG crystal (0.1 at. %, 7 mm length) to perform signal processing in this scenario.

Figure 3 (a) shows the RF spectrum of a broadband noise source (trace (i)) and that of the input codes from the PPG that mimicked a radar return signal at three levels of signal attenuation (0 dB in trace (ii), 15 dB in trace (iii) and 30 dB in trace (iv)). The return signal was attenuated and summed with the noise signal, and subsequently applied to the EOPM. Figure 3 (b) shows the SNR of the processed signal peak after 750 shots at 1 Gb/s (512 bits PN codes) as a function of the attenuation of the signal strength. For example, the last point of Figure 3(b) at 30 dB of signal attenuation corresponds to the case when the signal in (i) was summed with the signal in (iv) of Figure 3(a). Observed is a 1dB/dB drop in the processed result for attenuated signals (at low power), as expected, and this behavior is observed even in the presence of significant additive broadband noise.

V. VARIABLE DELAY PROCESSING OVER 5.0 MICROSECONDS

Figure 4 shows the results of processed time delays that were varied from approximately 0.7-5.9 μs and were extracted from corresponding spectral gratings recorded in Tm:YAG (0.1 at. %, 7 mm length). The gratings were created with 1 Gb/s codes repeated for 200 shots, and read out with a 200 MHz chirp as illustrated in Figure 2. The figure shows normalized peak strength as a function of the time delay.

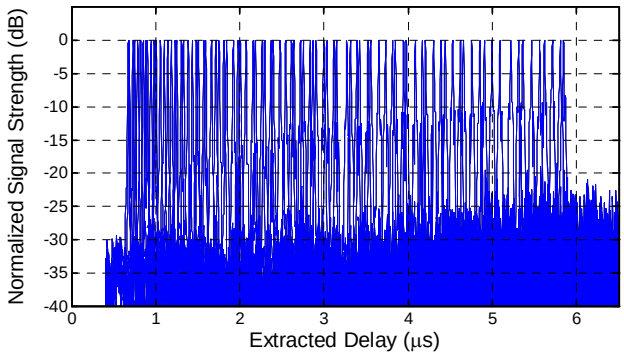

Fig. 4. Variation of processed delays over a 5.0 μs time aperture. The processed signals are normalized to remove the signal strength loss of ~2 dB/μs for this material, but show that the SNR does not decrease substantially (~1dB/μs) over this variation.

Under these conditions, the root-mean-squared noise background was observed to grow at ~1 dB/μs, thus demonstrating a substantial time aperture.

VI. 1 and 10 Gbps Material Coherence Measurements

An important feature of an AOSP is the coherent time-aperture over which it will operate, which essentially determines the maximum delay which can be processed and still provide a suitable signal-to-noise on the output signal. In S2 materials, the resultant signals from an AOSP operation will decay exponentially due to the material characteristics as a function of many factors including temperature, dopant density, excitation bandwidth, optical intensity per exposure and number of exposures.

Absorbing ions can influence the resonance characteristics of spatially located neighbors in the host lattice through dipole interactions which contribute to atomic decoherence. As the dopant concentration is lowered ions are spatially located further from each other, decreasing these interactions. Optical power has a similar influence on interactions, since the number of excited ions directly depends on the photon fluence.

A systematic dependence of the material coherence time was performed while varying the dopant density, optical power and number of exposures. To demonstrate high bandwidth processing capability of this material, the baseband code bit rate was varied between 1 Gb/s (512 bit codes) and 10 Gb/s (5120 bit codes) with a fixed optical power. In these measurements, the broadband grating was probed with a brief pulse, resulting in a stimulated photon echo whose intensity was measured to decrease over the varied time delay aperture.

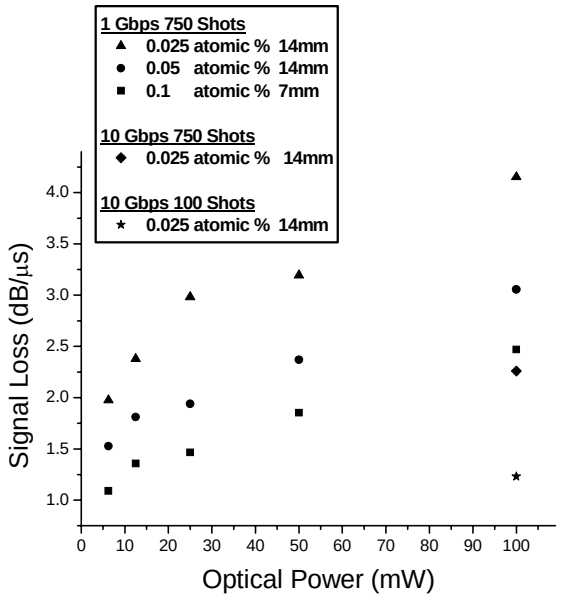

Fig. 5 Material signal loss measurements, in dB/μs at varying optical irradiation power, dopant concentrations, excitation bandwidth and number of shots. Values approaching 1 dB/μs are observed.

Figure 5 shows the effective signal loss in dB/μs as a function of the applied power and the dopant density of the material for various conditions. An increased signal loss is noted for both increased dopant density and increased optical excitation power. For the cases of 10 Gb/s modulation in the lowest dopant density sample (Tm:YAG, 0.025 at. %, 20 mm length), the effect of decreased signal loss with decreased shots is observed. Notably, for the case of 10 Gb/s modulation in this sample with 100 shots, there was a signal loss of ~1 dB/μs. A processing time bandwidth product of ~5000 and an effective time-aperture bandwidth product of 140,000 (~14 μs at 10 Gb/s) were thus demonstrated, which is to our knowledge, the highest values reported in optical signal processing applications. A detailed study on the high bandwidth processing capabilities of the SS based analog signal processor will be reported in a future publication.

VII. Conclusion

In summary, features of an wideband analog optical signal processing technique using a currently available S2 material, Tm:YAG, have been experimentally demonstrated. These demonstrations used a frequency stabilized continuous wave laser, commercially available telecom components, and a low-power optical chirped pulse probe. The capabilities demonstrated here represent substantial progress towards a practical, high performance, multi-GHz, analog coherent integrating temporal processor based on S2 materials.

References

[1] R.H. Walden, “Analog-to-digital converter survey and analysis,” IEEE Journal on Selected Areas in Communications, vol. 17, no. 4, pp. 539-550, April 1999.

[2] F. Stroili, J. Huggett, D. Jansen, R. Elder, D. Rowe, M. Vadipour, R. Chan, M. Feng, “Multifunction Receiver-on-Chip Technology for Electronic Warfare Applications”, Proceedings of GomacTech2004, Monterey, CA (2004).

[3] W. Cheng, R. Stevens, F. Rupp, C. Engels, W. Ali, M. Choi, D. Devendorf, S. Ding, L. Linder, K. Liu, T. Tat “40 GSPS ADC-DAC Components for the ADAM Receiver-Exciter ASIC, Proceedings of GomacTech2004, Monterey, CA (2004).

[4] Z. Cole, T. Böttger, R. Krishna Mohan, R. Reibel, W. R. Babbitt, R. L. Cone and K. D. Merkel, “Coherent integration of 0.5 GHz spectral holograms at 1536 nm using dynamic bi-phase codes,” Appl. Phys. Lett. 81, 3525 (2002).

[5] K. D. Merkel, R. Krishna Mohan, Z. Cole, T. Chang, A. Olsen and W. R. Babbitt, “Multi-Gigahertz radar range processing of baseband and RF carrier modulated signals in Tm:YAG,” J. Lum. 107 62-74 (2004).

[6] R. Reibel, Z. Barber, J. Fischer, M. Tian, W. R. Babbitt, “Broadband demonstrations of true-time delay using linear sideband chirped programming and optical coherent transients,” J. Lum. 107, 103-13 (2004).

[7] L. Levin, “Mode-hop-free electro-optically tuned diode laser,” Opt. Lett. 27, 237-29 (2002).

[8] T. Chang, R. Krishna Mohan, T. L. Harris, M. Tian, W. R. Babbitt, and K. D. Merkel, “Bridging the gap between absorption spectroscopy and optical coherent transient spectroscopy,”, manuscript submitted to Phys. Rev. A (2004)

[9] N. M. Strickland, P. B. Sellin, Y. Sun, J. L. Carlsten, and R. L. Cone, “Laser frequency stabilization using regenerative spectral hole burning,” Phys. Rev. B 62, 1473 (2000).

[10] R. R. Reibel, Z. W. Barber, M. Tian, W. R. Babbitt, Z. Cole, K. D. Merkel, “ Amplification of high-bandwidth phase-modulated signals at 793 nm” J. Opt. Soc. Am. B 19 2315 (2002).